



# Flexural Performance of Prefabricated Composite Girders along with Precast Deck-to-Girder Continuous Connections

Byung H. Choi<sup>1</sup> · Hung Thanh Diep<sup>1</sup> · Jiho Moon<sup>2</sup>

Received: 10 July 2023 / Accepted: 21 December 2023 / Published online: 17 January 2024  
© Korean Society of Steel Construction 2024

## Abstract

Recently, a great amount of research has been carried out to resolve a growing need for durable and resilient highway bridge construction/reconstruction systems in many countries. As a part of such studies, prefabricated composite girders with innovative precast deck-to-girder continuous connections have been proposed that facilitate construction by eliminating interference during on-site processes. This study aims to figure out the effects on the flexural performance of the prefabricated composite girders along with the non-interference deployment of the precast deck-to-girder interface connections. In this study, two test specimens of the prefabricated composite girder were designed. Ultimate bending tests were conducted to experimentally evaluate the behavior of shear interfaces and flexural performances of the test specimen girders. It was revealed from this study that the intersection of the lap connection between the transverse deck reinforcement and the shear connectors will have a significant effect on the flexural performance of the prefabricated composite girder. The flexural performance of the prefabricated composite girder with intersected connection type is ensured while the non-intersected connection type influences the flexural performance more seriously than the intersected connection type. The AASHTO LRFD specifications appears applicable to the existing intersected connection details. Further, a series of parametric studies based on the verified finite element model were performed to examine the influence of various dominant factors on the flexural moment strength of the prefabricated composite girder. From the results of parametric studies, conclusions were drawn. The results of this study could be used for future research to establish a procedure for evaluating the bending resistance capacity of prefabricated composite girders based on structural ductility through rotating capacity.

**Keywords** Contact finite element analysis · Experimental bending test · Flexural performance · Prefabricated composite girder · Precast deck-to-girder connection

## 1 Introduction

Prefabricated bridge girders deployed countless times in highway infrastructure are reliable and common structural members. In the most popular form, these prefabricated bridge girders and the cast-in-place concrete deck are connected using discrete shear connectors either welded onto or cast into the girders. The on-site construction of such a deck

system is fairly straightforward, but progress can be slow because of the need to perform field operations related to the casting and maintenance of the deck concrete. Thus, there is interest in utilizing prefabricated bridge deck elements to speed up on-site construction activities and improve the quality of the deck concrete. For this reason, prefabricated bridge deck elements are continuously employed. To accelerate construction, prefabricated bridge deck elements have been used since the 1970s (Haber & Graybeal, 2018). The initial deployment was primarily used in deck replacement projects when rapid project delivery was required, to reduce interference with local traffic in densely populated areas. Prefabricated bridge deck elements have since been studied extensively in both field inspection studies, and laboratory investigations (Biswas, 1986; Tawadrous & Morcou, 2018). The first factor influencing the performance of prefabricated bridge deck elements is the connection material. The ideal

---

✉ Hung Thanh Diep  
dthung@hanbat.ac.kr

<sup>1</sup> Department of Civil and Environmental Engineering, Hanbat National University, Yuseong-Gu, Daejeon 34158, Republic of Korea

<sup>2</sup> Department of Civil Engineering, Kangwon National University, Chuncheon-Si, Gangwon-Do 24341, Republic of Korea

material is rapid strength gain, dimensional stability, good workability, good durability properties, and good bond to precast concrete. Previous research on grout materials has mainly concentrated on new properties, constructability aspects, durability, bond strength to precast concrete, and dimensional stability (Zhu & Ma, 2010). The next factor is the surface preparation at the connection location. It is proven that the surface roughness of the precast concrete greatly affects the bond between the connection material and the precast concrete (Abu-Tair et al., 1996; Momayez et al., 2005; Santos et al., 2007). (De La Varga et al., 2017) gave a similar conclusion. The final factor is the connection details between components. In several prefabricated bridge deck types, the full-depth deck panel system with clustered stud connectors in shear pockets is an expected type. However, when utilizing clustered stud connectors such as the shear connection, it is necessary to solve many problems, which consist of nonuniform shear stress distribution, local bearing failure of grout in the shear pockets, and deck uplift (Badie et al., 2010; Ovuoba & Prinz, 2018). Continuous void connections are a potential solution to be used instead of such point connections. (Graybeal, 2012) suggested composite girders with precast concrete girders connected to prefabricated deck panels through an injection channel. His study focused mainly on the connection type where the injection channel is filled with UHPC. Tests were also carried out to examine the connection performance and the bending behavior. From such a series of studies, prefabricated composite girders have been proposed in this study which can be readily and efficiently connected by mechanically injecting grout mortar through a continuous channel in between the steel girders and deck panels, as shown in Fig. 1. With the use of steel girders, the upper flange was made to be U-shaped so that it could serve as a formwork for grouting. Such connection of prefabricated composite girders is typically made by means of shear connectors placed within a partial depth block-out in the deck panels. This type of block-out solved concerns about durability compared to a full depth block-out, since the full depth block-out has exposed joints around the perimeter of the block-out after the grout is placed. The top deck reinforcement can be placed over the block-out,

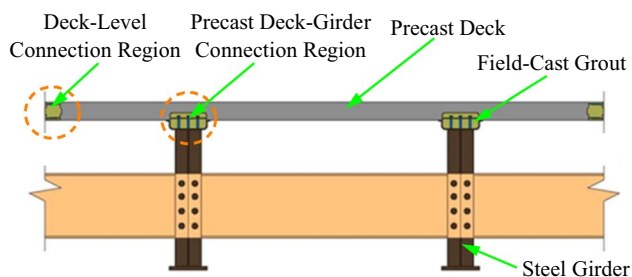


Fig. 1 Concept of prefabricated composite girders

which simplifies the layout of reinforcement in the deck panel. In addition, the continuous connection will allow more closely spaced shear connectors, and uniform shear stress distribution. Greater haunch height can be advantageous for the flow of grout under the deck panels and adjustment during precast deck module installation and connection. Because of such outstanding advantages, this type of connection needs more research attention to accelerate its applicability. From such a proposal, two test specimens of the prefabricated composite girder were designed. Ultimate bending tests were conducted to experimentally evaluate the behavior of shear interfaces and flexural performances of the test specimen girders. To evaluate flexural performances, the flexural moment strengths of the test girder specimens were compared with the nominal flexural resistances calculated from the equations (based on the current AASHTO LRFD (2020)) proposed by (Diep et al., 2022). Further, a series of parametric studies based on the verified finite element model were performed to examine the influence of various dominant factors on the flexural moment strength of the prefabricated composite girder.

## 2 Experimental Study

### 2.1 The Design of the Precast Deck-to-Girder Continuous Connection

The design of the precast deck-to-girder continuous connection includes three critical interface types, as indicated in Fig. 2: (1) Monolithic grout interface, (2) Interface between the precast deck and the field-cast haunch, and (3) Interface between the steel girder and the field-cast haunch. There are two different types of connection: The conventional connection (Shear connector and reinforcement intersect), and the non-intersected connection (Shear connector and reinforcement do not intersect). These two types are different in the monolithic grout interface. For the conventional connection, the shear strength of the monolithic grout interface is reinforced by reinforcements (1A & 1B) or shear connectors (1C). For the non-intersected connection, the shear strength of the monolithic grout interface includes only the shear strength of grout. The failure of the monolithic grout interface is at the interface corresponding to the minimum shear strength of interfaces (1A), (1B), & (1C).

The design of shear interfaces shall satisfy (Article 5.7.4.3 in the AASHTO LRFD):

$$v_{ui} \leq v_{ri} = \phi v_{ni} \quad (1)$$

where:

$v_{ui}$ : Factored interface shear stress.

$v_{ni}$ : Nominal interface shear resistance.

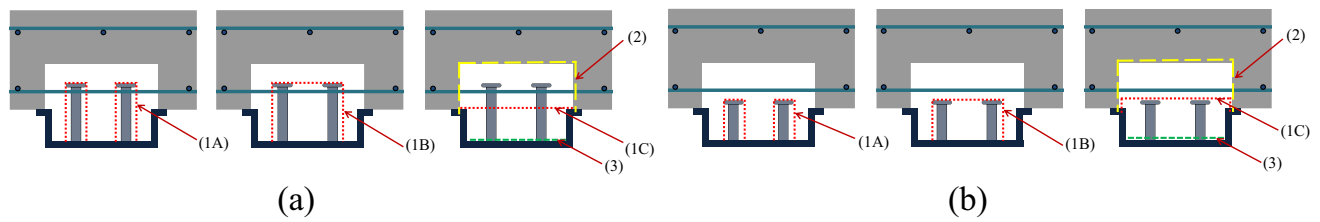


**Fig. 2** Shear planes of the precast deck-to-girder continuous connection: **a** Conventional connection: Shear connector and reinforcement intersect, and **b** Non-intersected connection: Shear connector and reinforcement do not intersect

$\phi$ : Resistance factor for shear.

$v_{ri}$ : Factored interface shear resistance.

The factored interface shear force per unit length ( $V_{ui}$ ) (Article C5.7.4.5 in the AASHTO LRFD):

$$V_{ui} = \frac{V_u}{d_v} \tag{2a}$$

where:

$V_u$ : Factored vertical shear force.

$d_v$ : Distance between the mid-thickness of the deck and the centroid of the bottom flange.

The factored interface shear stress ( $v_{ui}$ ) is calculated using the equation:

$$v_{ui} = \frac{V_u}{b_{vi}d_v} \tag{2b}$$

where:

$b_{vi}$ : The width of the interface.

In addition, from the mechanics of materials, the interface shear force per unit length ( $V_{ui}$ ) can be determined from the equation:

$$V_{ui} = \frac{V_u Q}{I} \tag{3a}$$

where:

$V_u$ : Factored vertical shear force.

$Q$ : First moment with respect to the neutral axis of the area of the cross-section beyond the interface of interest.

$I$ : Moment of inertia of the composite section.

Similarly, the interface shear stress ( $v_{ui}$ ) can be determined utilizing the equation:

$$v_{ui} = \frac{V_u Q}{b_{vi}I} \tag{3b}$$

The two equations appear to be quite different from one another, and a designer could, understandably, be confused as to which should be used. In fact, the two equations are closely related.

According to the AASHTO LRFD (Article 5.7.4.3), the nominal interface shear resistance ( $v_{ni}$ ) is calculated as follows:

$$v_{ni} = c + \mu(\rho f_y + N)$$

$$v_{ni} \leq K_1 f_c' \tag{4}$$

$$v_{ni} \leq K_2$$

where:

$c$ : Cohesion factor.

$\mu$ : Friction factor.

$\rho$ : Interface shear reinforcement ratio ( $= A_{vf}/A_{cv}$ ).

$N$ : Permanent net compressive stress ( $= P_c/A_{cv}$ ).

$A_{vf}$ : Area of shear reinforcement crossing the interface.

$A_{cv}$ : Area of concrete section resisting shear transfer.

$P_c$ : Permanent net compressive force normal to the shear plane.

$f_y$ : The reinforcement yield stress.

$f_c'$ : The compressive strength of concrete.

$K_1$ : Fraction of concrete strength available to resist interface shear.

$K_2$ : Limiting interface shear strength.

(Diep & Choi, 2023) evaluated the design provisions for interface shear resistance and concluded that the AASHTO LRFD is most appropriate when calculating shear resistance for monolithic and roughened interfaces.

The design of the interface between the steel girder and the field-cast haunch for the prefabricated composite girder is similar to that for a conventional composite girder provided in the AASHTO LRFD (Article 6.10.10). Note that the form of design equations in the AASHTO LRFD is unified to stress-based.

Generally, if the above design equations of the connection are satisfied, the condition of full shear connection for the composite girder can be ensured. To understand the new connection behavior and evaluate the flexural performance of the prefabricated composite girder, experimental

and simulation investigations were carried out, since the AASHTO LRFD did not provide equations to determine the shear strength of monolithic grout and precast concrete-to-grout interfaces.

### 2.2 Specimen Design

As presented in Sect. 2.1, there are two types of connections which are conventional and non-intersected connections with their different behavior. Therefore, it is necessary to design both test specimens with such two connection types. These two specimens were fabricated to examine the flexural performance through moment strength by a typical 3-point bending test. Each specimen is 968 mm high and 6,400 mm long. The precast deck is 860 mm wide  $\times$  6,400 mm long  $\times$  220 mm thick. Specimen 1 was designed with conventional connection (CC specimen): Shear connector and

reinforcement intersect with the height of the shear connector of 150 mm. Specimen 2 was designed with non-intersected connection (NC specimen): Shear connector and reinforcement do not intersect with the height of the shear connector of 110 mm. In general, these two specimens only differ in the height of the shear connector. The shear connector has a diameter of 19 mm. Both specimens were loaded statically to failure. Figure 3 indicates the general details of the test specimens.

The steel girder and stiffeners apply the structural steel HSB380. The yield strength and ultimate tensile strength of the shear connector are (380 & 420) MPa, respectively. The yield stress of reinforcement is 400 MPa. For the CC specimen, the measured compressive strength of the precast concrete and grout is (16.85 & 36.61) MPa, respectively, while that of the NC specimen is (17.66 & 42.30) MPa, respectively.

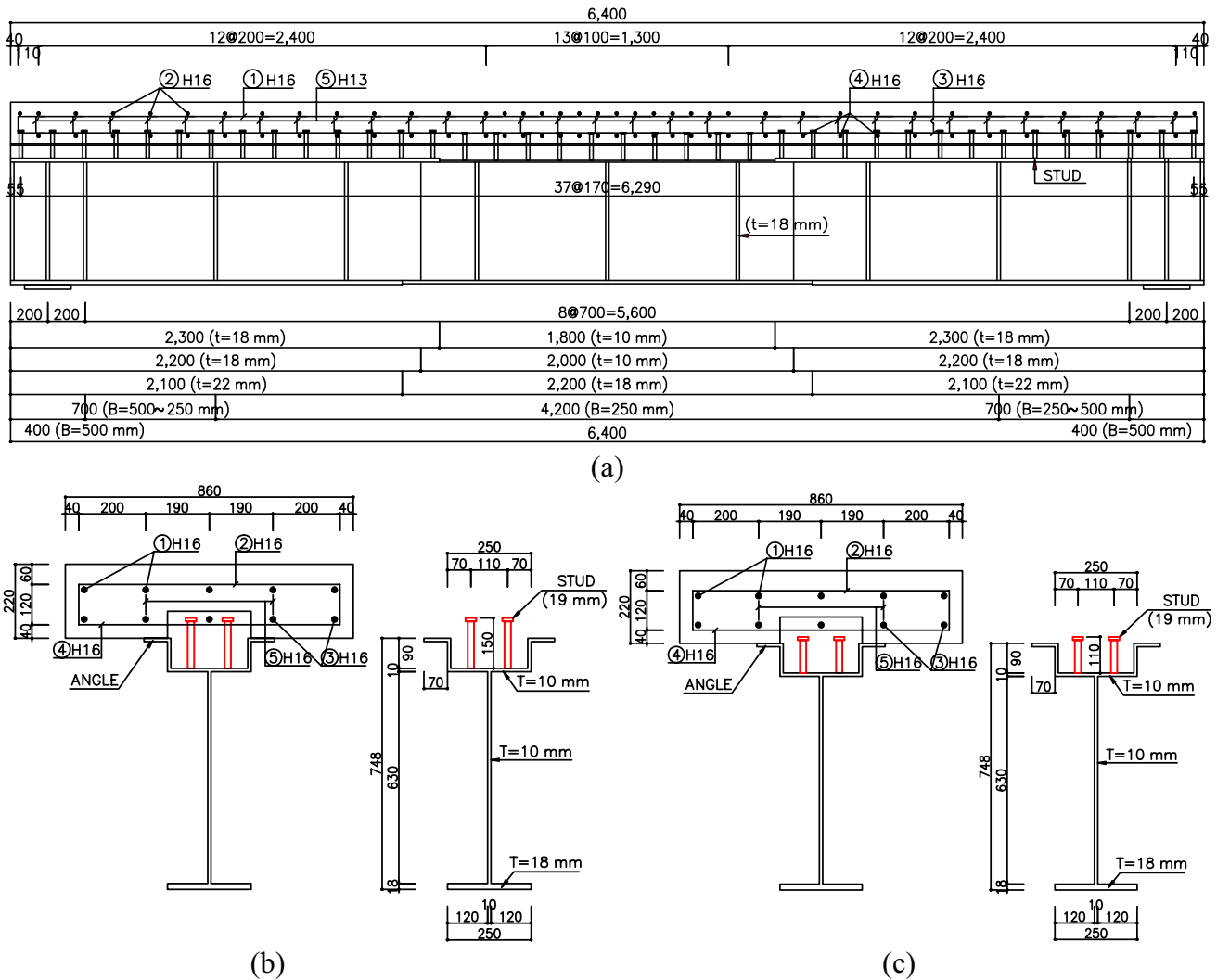


Fig. 3 General details of test specimens: **a** Elevation view, **b** Cross section (CC specimen), and **c** Cross section (NC specimen)

### 2.3 Instrumentation and Test Set-Up

Figure 4a indicates the test setup utilized in this study. As illustrated in Fig. 4b, linear variable displacement transducers (LVDTs) were utilized to measure the vertical displacements, and strain gauges were installed to monitor the normal strains of the prefabricated composite girder models. LVDTs were also installed to monitor the slip of connection at the end of the prefabricated composite girder.

## 3 Results and Discussions

### 3.1 Test Results (CC specimen)

Figure 5a shows the relationship between the moment ratio and the displacement for the CC specimen. In Fig. 5a, the  $y$  axis denotes the applied moment to the nominal flexural resistance ( $M_n$ ) ratio, while the displacement is denoted on the  $x$  axis. The test result shows that when the bottom of the steel girder yielded ( $M_y$ ), the stiffness was noticeably decreased. The flexural moment strength of 3,243.74 kNm ( $M_{u,test}$ ) was observed at the deflection of 66 mm. The nominal flexural resistance of the test specimen calculated from the equations proposed by (Diep et al., 2022) is 2,531.41 kNm. Therefore, the proposed equations underestimated the flexural moment strength by approximately 21.96%. The

flexural performance of the prefabricated composite girder was ensured.

Figure 5c shows the strain distributions at the ultimate mid-span deflection. These strain distributions after the test show that the strain exceeded the yield strain ( $\epsilon_y=0.002215$ ) at the bottom of the steel girder. The strains of the concrete surface and rebars were less than those of the steel girder. In addition, strain distribution was discontinuous at the interface between the connection grout and the steel girder. The slip at the interface is the cause of this, and implies that the interaction behavior at the connection of the test specimen is partial interaction behavior. While there was no shear connector failure during the test, the crack and slip between the steel girder and the connection grout were observed. Figure 5d indicates the crack and slip at the end of the specimen. Despite discontinuous strain distribution, the full shear connection can be ensured, since the whole concrete deck and connection grout undergo compression, and only one neutral axis is observed in the composite section. In general, when only one neutral axis is observed in the composite section, the full shear connection can be ensured, regardless of the degree of interaction (Cho et al., 2018; Oehlers & Bradford, 1995).

Figure 5b provides the load–slip relationships obtained for the test specimen. This figure shows that slip was observed at both the haunch-to-steel girder and the deck-to-haunch interfaces. At the peak load, the haunch-to-steel

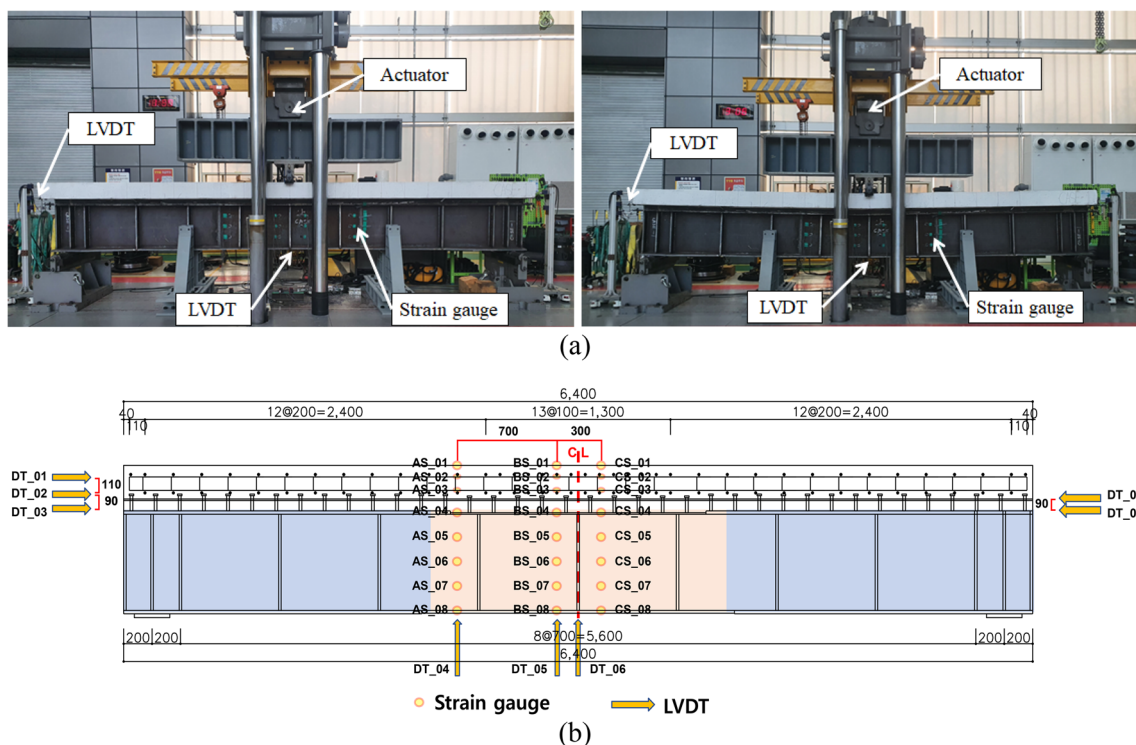
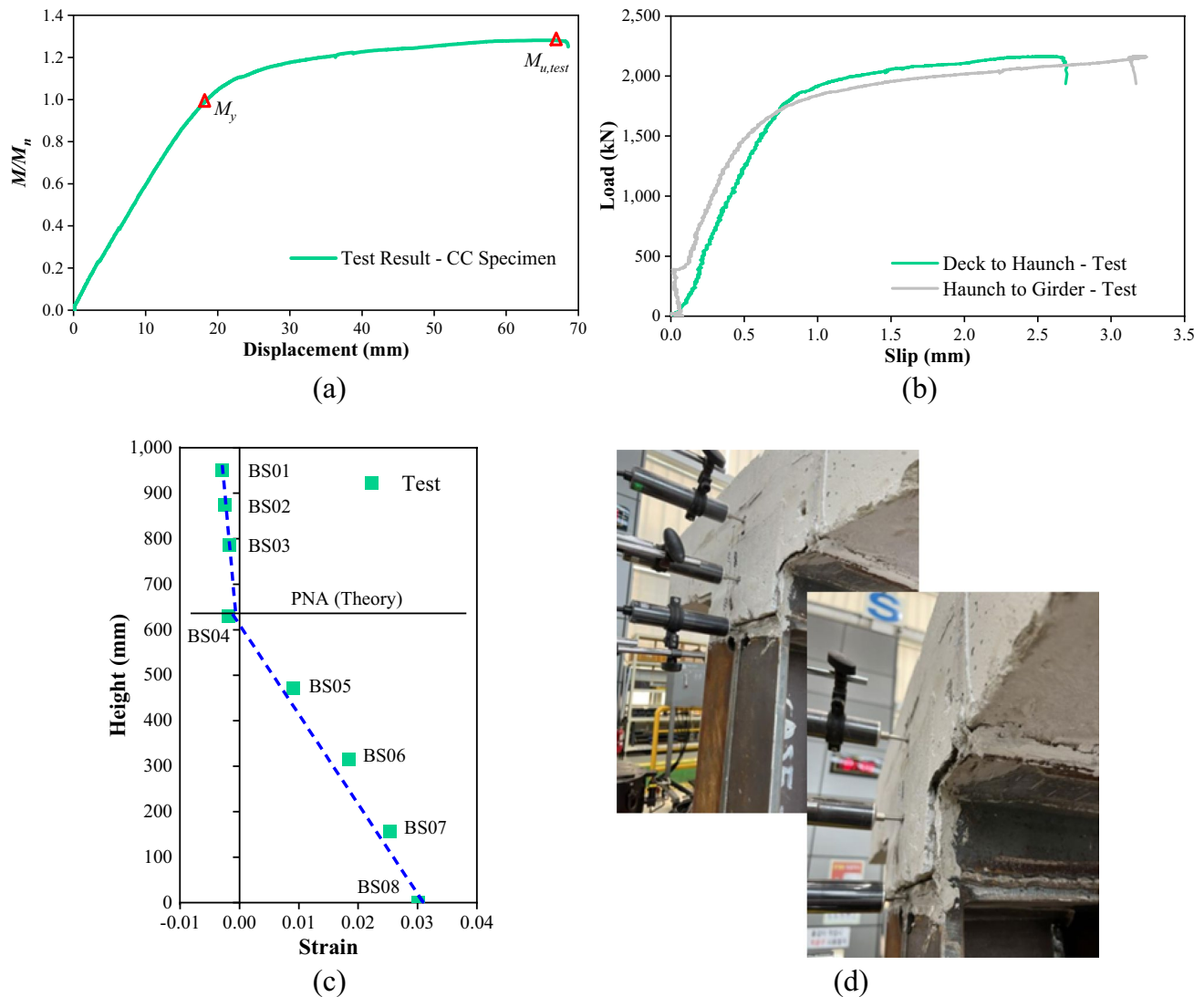


Fig. 4 Test setup and arrangement of instrumentation: a Test setup for CC & NC specimen, and b Arrangement of instrumentation



**Fig. 5** Test results (CC specimen): **a** The moment ratio–displacement curve, **b** The load–slip relationships, **c** The strain distribution over the beam depth, and **d** The slip mode shape

girder interface slip and the deck-to-haunch interface slip were (3.27 & 2.65) mm, respectively.

Figure 5d shows the slip mode at the connection obtained for the test specimen. No slip was observed at the horizontal interface between the precast deck and the haunch. This interface remained uncracked through the global failure of the test specimen. All slips occurred at the haunch-to-steel girder interface. This is in contrast to the slip provided in Fig. 5b. But note that the distance of the slip measurement points between the precast deck and the haunch is greater than that between the steel girder and the haunch. When the prefabricated composite girder is bent, the horizontal displacement is different between the two measuring points of the deck and the haunch, although there is no actual slip between the deck and the haunch. This is also consistent with the load–slip curve, which shows that initially, the slip

between the deck and the haunch is greater than that between the steel girder and the haunch, but then is the opposite. Due to the intersection of reinforcement and shear connector, there is no cracking at the monolithic grout interface.

In general, there was no failure at the connection, and the flexural performance of the prefabricated composite girder with conventional precast deck-to-girder continuous connection was ensured.

Note that the factored interface shear resistance of 3.586 MPa calculated from Eq. (4) with additional consideration of the resistance factor ( $\phi=0.9$ ) is greater than the required interface shear resistance of 3.203 MPa calculated from Eq. (3b) through the test load ( $P_{test}=2,162.49$  kN). Therefore, the AASHTO LRFD appears applicable to the conventional precast deck-to-girder continuous connection. The interface that governs this conventional connection of

the prefabricated composite girder is the interface between the precast deck and the field-cast haunch (2).

### 3.2 Test Results (NC specimen)

Figure 6a indicates the moment–displacement curve for the NC specimen. The test result shows that the flexural moment strength of 2,971.40 kNm was observed at the deflection of 27 mm. The plastic moment of the test specimen calculated from the proposed equations by (Diep et al., 2022) is 3,041.83 kNm. The flexural moment strength has not reached the plastic moment; the connection has failed.

Figure 6b illustrates the failure mode shape at the connection. Cracks began to appear on the test specimen at the connection. The final collapse of the prefabricated composite girder was caused by the failure of the connection. In particular, it is the shear plane (1C). This is the shear plane corresponding to the minimum shear strength of the monolithic grout interfaces.

In general, the non-intersected connection type seriously influences the flexural performance of the prefabricated composite girder, which is expected to be evaluated in detail in future studies, in comparison with the conventional connection type where the approximately equal compressive strength of grout is used.

## 4 Finite Element Model

In this study, to appropriately simulate the shear interfaces based on the test results and set up the verified model for parametric studies, finite element analysis (FEA) of the test specimens using ABAQUS (2020) was conducted. Figure 7a shows the model of the test specimen including 5 components: steel girder, connection grout, concrete deck, shear connector, and rebar. The element types used for the model are the solid element C3D8R, the shell element S4R, and the truss element T3D2, as shown in Fig. 7b. The fine and

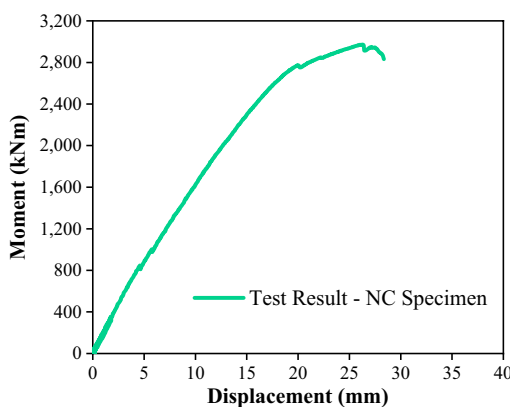
overall mesh (size of 50–100 mm, respectively) is applied to the appropriate parts to obtain accurate results and reduce analysis time. Especially, size of the shear connector was (3–5) mm because of its small dimension.

The interaction between components was considered utilizing appropriate interactions and constraints at each location including tie constraint, embedded constraint, friction interaction, and cohesive interaction, as shown in Fig. 7c. The friction factor in friction interaction between connection grout and steel girder was 0.3 (Baltay & Gjelsvik, 1990; Diep et al., 2023). For cohesive interaction, uncoupled stiffness coefficients ( $K_{nn}$ ,  $K_{ss}$ ,  $K_{tt}$ ), peak values of traction ( $t_n^0$ ,  $t_s^0$ ,  $t_t^0$ ), and an effective separation at complete failure ( $\delta_m^f$ ) are used to simulate cohesive failure between surfaces of connection grout and concrete deck. In this study, different values of these parameters were tried to select based on the best fit of moment–displacement curves between the analysis and the test results. As a result, the values of these parameters are as follows:  $K_{nn} = K_{ss} = K_{tt} = 4$ ,  $t_n^0 = t_s^0 = t_t^0 = 4$ , and  $\delta_m^f = 5$ . Note that these parameters were selected based on the best fit of moment ratio–displacement curves between the analysis and the test results, and so that damage does not occur at this interface for both CC Specimen and NC Specimen. The parameters resulted in the same outcome for the CC and NC specimens. Therefore, the reliability of the test, as well as the FEA, was increased.

A typical 3-point bending test analysis was carried out to investigate the flexural performance of the test specimens through their flexural moment strength. The distance between the end of the girder and the loading point is 3,200 mm. The hinge support was used to restrain displacements of the prefabricated composite girder in the Z direction, while the roller support was used so that the prefabricated composite girder could be freely moved in the Z direction.

Figure 8a indicates the stress–strain relationship for precast concrete. For the precast concrete in compression, the stress–strain curve was adopted according to the

**Fig. 6** Test results (NC specimen): **a** The moment–displacement curve, and **b** The failure mode shape at the connection



(a)



(b)

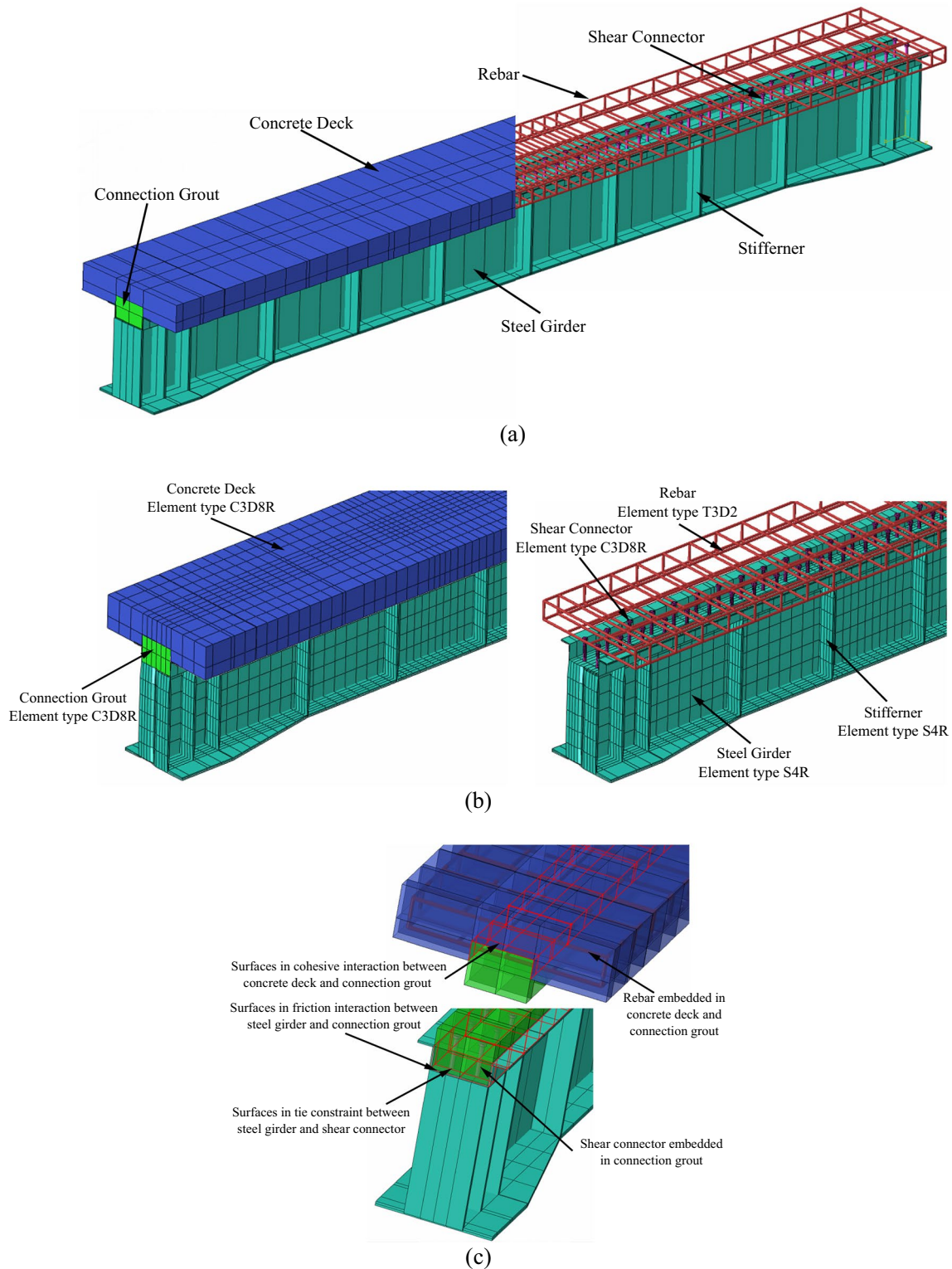


**Fig. 7** Model of the prefabricated composite girder: **a** Model, **b** Finite element type and mesh, and **c** Constraint and interaction surfaces

study of (Hognestad, 1951). Equation (5) is used to calculate the initial Young's modulus ( $E_c$ ). Equations (6a) and (b) are used to simulate the variation of nonlinear

segments, respectively. For the precast concrete in tension, the bi-linear curve was applied (Chen, 1982).



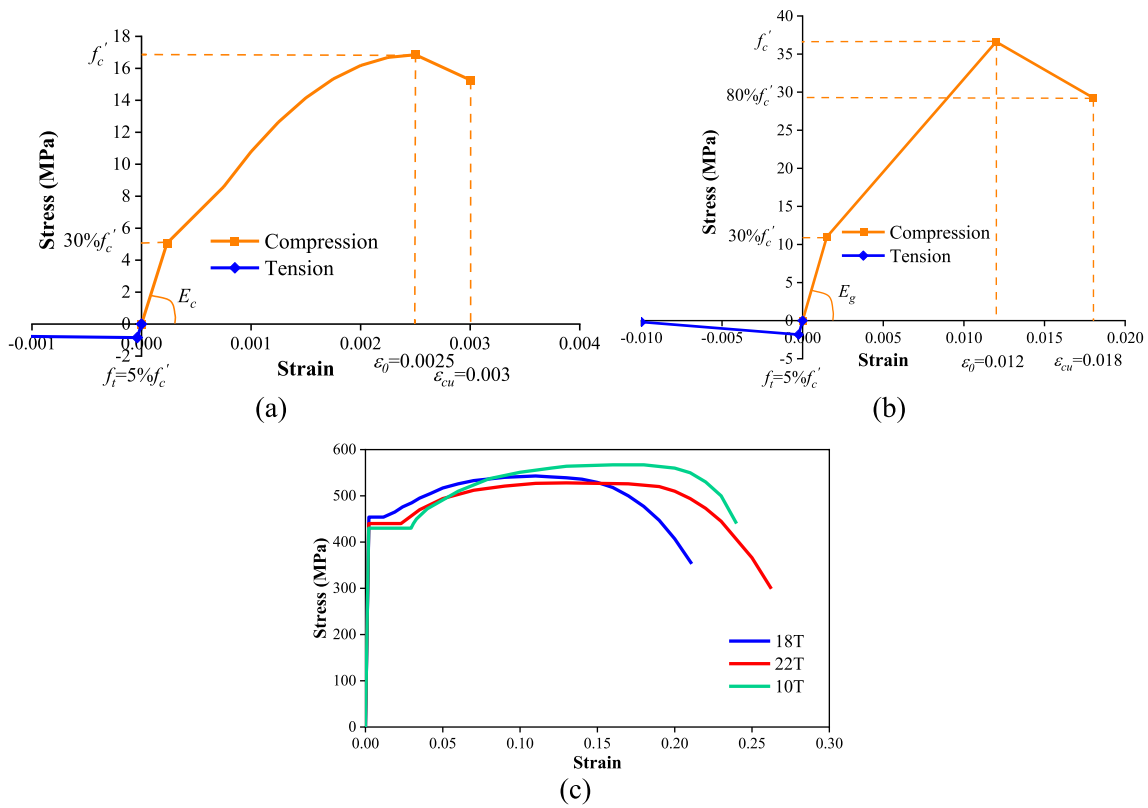


Fig. 8 Stress–strain relationship for materials: **a** For precast concrete, **b** For grout, and **c** For structural steel

$$E_c = 8,500 \times (f_c')^{1/3} \tag{5}$$

$$f_c = f_c' \left[ 2 \frac{\epsilon_c}{\epsilon_0} - \left( \frac{\epsilon_c}{\epsilon_0} \right)^2 \right] \tag{6a}$$

$$f_c = f_c' \left[ 1 - \frac{0.15}{0.003 - \epsilon_0} (\epsilon_c - \epsilon_0) \right] \tag{6b}$$

For the grout in compression, the stress–strain curve (a tri-linear model) was adopted according to the study of (Kaushik et al., 2007). Equation (7) is used to calculate the elastic modulus of grout ( $E_g$ ) The tensile properties of grout are simulated to be similar to that of precast concrete. The stress–strain relationship of the grout material is shown in Fig. 8b.

$$E_g = 200 \times (f_c') \tag{7}$$

The structural steel HSB380 with different thicknesses applied the real stress–strain curve, as indicated in Fig. 8c. The shear connector and reinforcement steel applied the elastic–perfectly plastic curve.

## 5 Verification of the Finite Element Model

### 5.1 The CC Specimen

Figure 9a compares the flexural moment strength of the analysis result with that of the test. The analysis result agrees well with the test. From the FEA result, the finite element model underestimated the flexural moment strength by 0.77%. Additional finite element analysis was performed to examine the effect of the degree of interaction between the steel girder, precast concrete deck, and connection grout on the behavior of the prefabricated composite girder. To simulate the degree of interaction, two different interface models were used. The first interface model is a partial interaction model with a detailed simulation of the connection, as presented in Sect. 4. The other is a full interaction model by tie constraint to restrict all slip between the precast concrete deck, the steel girder, and the connection grout. Figure 9b compares the FEA results based on the degree of interaction. Figure 9b shows that the stiffness of the test girder modeled with partial interaction is slightly lower than that of the test girder modeled with full interaction. However, the flexural moment strength between these two models has a difference of only 1.00%. As a result, the effect of the degree of interaction between the steel girder, precast concrete deck, and

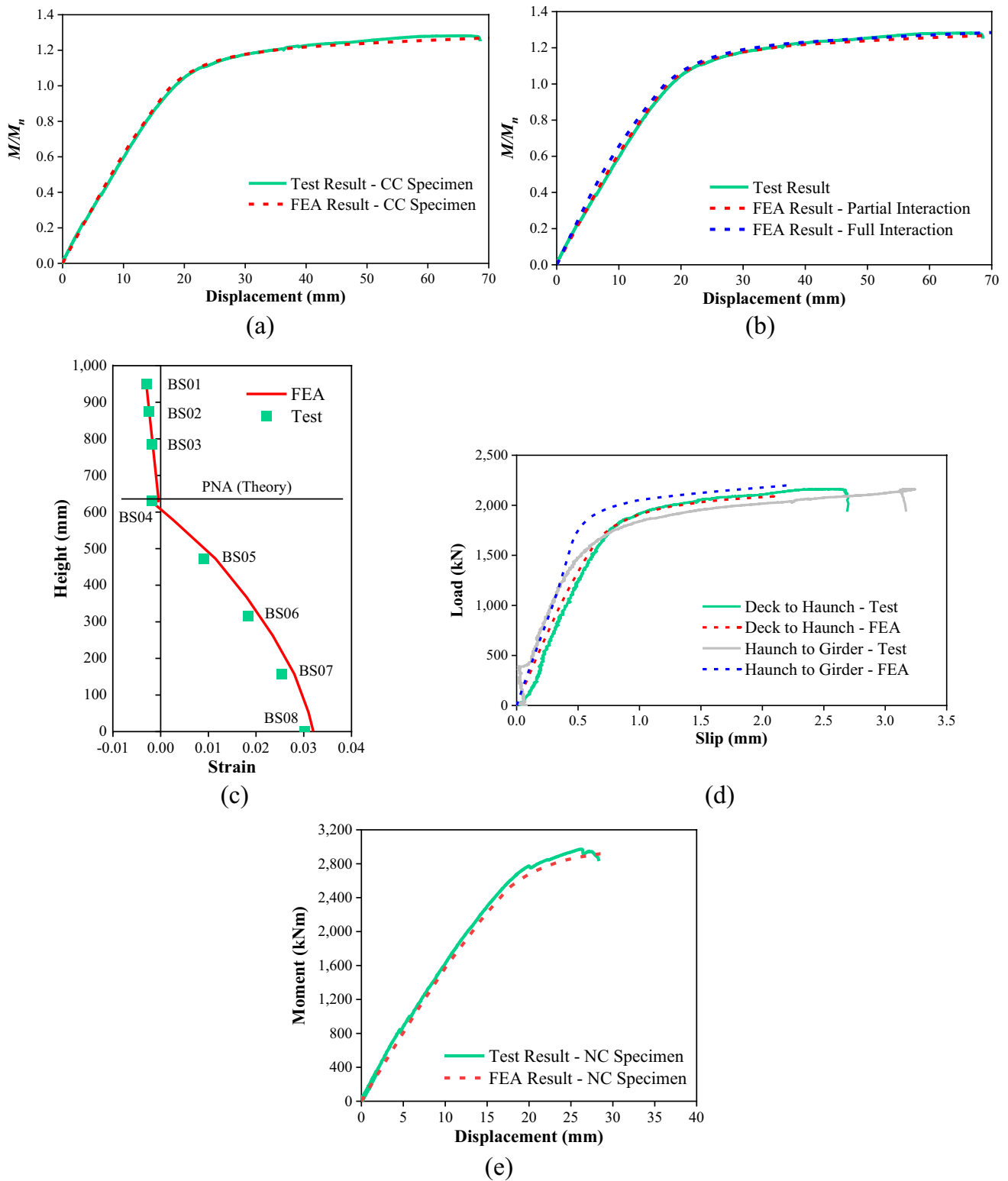


**Fig. 9** Comparison of the FEA result with test: **a** Comparison of flexural moment strength, **b** Comparison of flexural moment strength based on the degree of interaction, **c** Comparison of strain distribu-

tion, **d** Comparison of slip, and **e** Comparison of flexural moment strength (NC specimen)

connection grout was negligible, since the condition of the full shear connection was met for the test specimen.

Figure 9c shows the strain distributions along with the height in the BS section (at the peak load). The squares in Fig. 9c represent the strain obtained from the test, while the solid line represents the FEA result. The strain distributions obtained from the FEA agree well with those from the test, as indicated in Fig. 9c. In addition, the location of PNA obtained from the FEA was almost similar to that of the test result.

Figure 9d gives the distribution of interface slip. The maximum relative slip between the precast concrete deck and the haunch of the test and the FEA is (2.65 & 2.10) mm, respectively, with a high degree of coincidence. There is a difference in the slip between the haunch and the steel girder. But this difference can be eliminated due to the good fit of the moment ratio–displacement curve, as well as the strain contribution of the finite element model, compared with the test.

## 5.2 The NC Specimen

Figure 9e compares the analysis result with the test, and shows good agreement between the two. From the FEA result, the finite element model underestimated the flexural moment strength by 1.80%. The flexural moment strength has not reached the plastic moment; the connection has failed.

## 6 Parametric Study

As investigated, the flexural performance of the CC specimen was ensured. Parametric studies based on the verified finite element model of the CC specimen were performed to examine the influence of various dominant factors on the flexural moment strength of the prefabricated composite girder. The parameters consist of the compressive strength of concrete and grout, the thickness of upper and bottom flange, and the height of steel girder.

For the CC specimen, the measured compressive strength of concrete is 16.85 MPa. Different compressive strengths from 20 to 35 MPa are applied to the precast concrete deck in the parametric study models to provide insight into the influence of the compressive strength of concrete. Figure 10a indicates that the compressive strength of concrete has a certain degree of influence on the flexural moment strength of the prefabricated composite girder. Note that the change range in compressive strength of concrete is small and the location of the plastic neutral axis is around the haunch area so the effect of the compressive strength of concrete on the flexural moment strength is not significant. 0.78–2.70%

increase in the flexural moment strength is recorded over the investigated parameter range.

For the test girder, the connection grout has a compressive strength of 36.61 MPa. Various compressive strengths from 40 to 100 MPa are applied to the connection grout to consider the effect of the compressive strength of grout. Figure 10b shows that the flexural moment strength has an increase from 0.90% to 5.94% in the investigated parameter range of compressive strength of grout. It is also seen that the flexural moment strength is less sensitive when the compressive strength of grout becomes higher. Note that the compressive strength of grout up to 100 MPa, has a larger variation than the compressive strength of concrete and that the area of the grout in the case of test girders accounts for a large proportion of the total area of the concrete. The location of the plastic neutral axis is also around the haunch area, the effect of the compressive strength of grout on the flexural moment strength is not significant.

In the original model, the upper flange is 10 mm thick. Thicknesses from 14 to 22 mm are applied to the upper flange to provide insight into the influence of the thickness of upper flange. It can be observed from Fig. 10c that the upper flange thickness has a negligible influence on the flexural moment strength of the prefabricated composite girder.

The bottom flange has a thickness of 18 mm for the CC specimen. To investigate the influence of bottom flange thickness on the mechanical characteristics of the prefabricated composite girder, the thickness of bottom flange is replaced within the range of 14–26 mm. In Fig. 10 d, a 8.92% decrease is found in the model whose thickness of bottom flange is 14 mm while a 9.86% increase is corresponding to 22 mm thick bottom flange.

In this parametric study, various heights from 600 to 950 mm are applied to the steel girder. The displacement–moment curves are shown in Fig. 10e. It can be observed that the steel girder height has a noticeable influence on the flexural stiffness of the structure. And in the range of 600–950 mm, the effect of steel girder height on the flexural moment strength varies between -19.20 and 37.73% compared with the CC specimen whose steel girder is 748 mm high. It is illustrated that increasing the steel girder height is an effective method to improve the flexural moment strength.

The flexural moment strength comparison results are presented in Table 1. From the analysis results, the proposed equations (Diep et al., 2022) underestimated the flexural moment strength of the prefabricated composite girder by approximately 5.53–25.01%. The flexural performance of the prefabricated composite girder for all models was ensured.

In addition, for the NC specimen, the high strength grouts in the haunch are expected to significantly improve the interface shear strength, thereby ensuring the flexural performance of the prefabricated composite girder. 120–150 MPa compressive strengths of the grout are

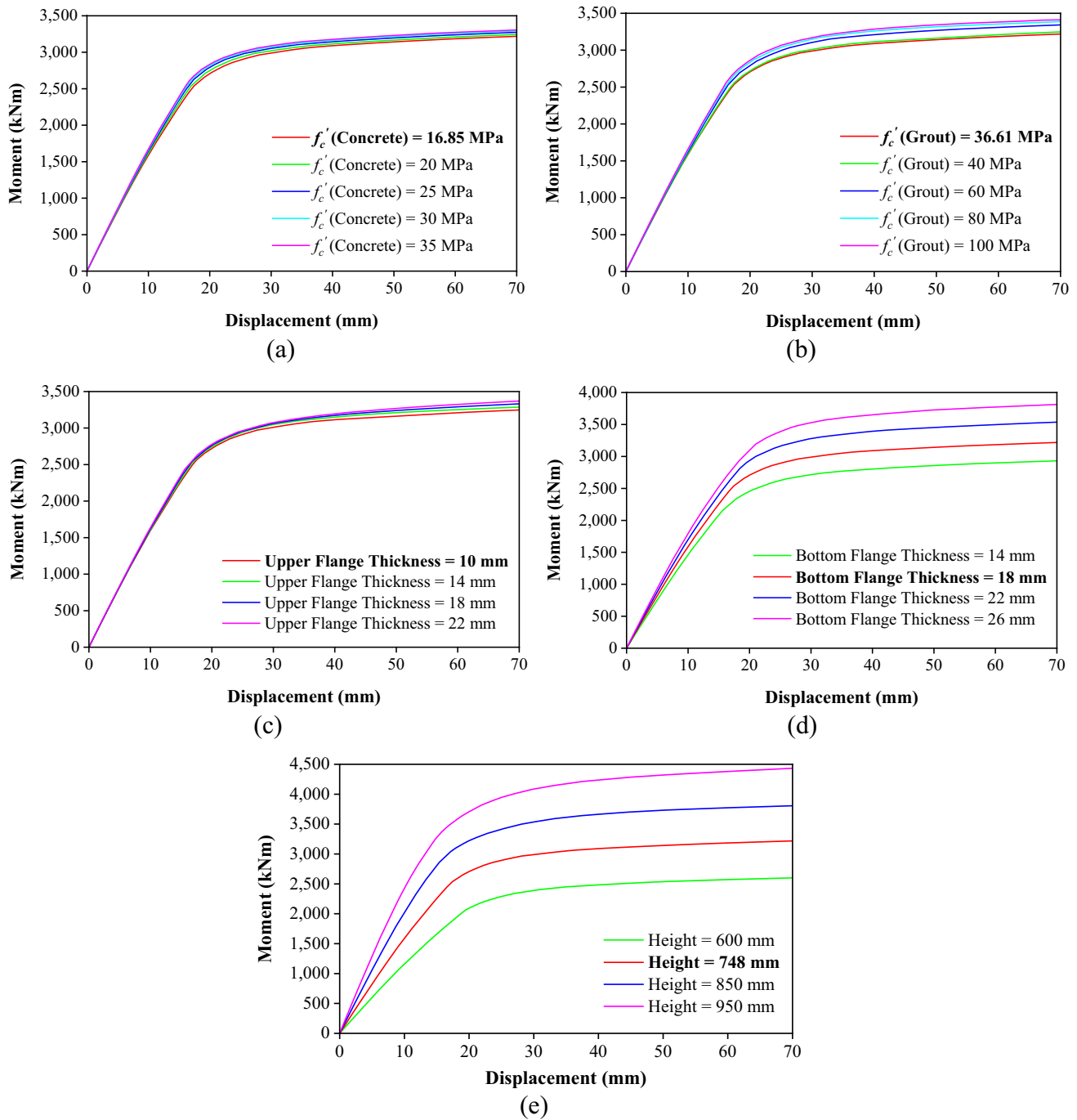


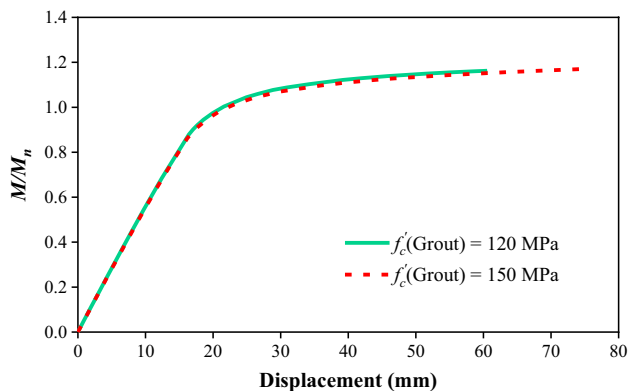
**Fig. 10** Effect of various dominant factors on the flexural moment strength: **a** The concrete compressive strength, **b** The grout compressive strength, **c** The thickness of upper flange, **d** The thickness of bottom flange, and **e** The height of steel girder

applied to the connection for the NC specimen to consider the effect of the compressive strength of grout. Figure 11 shows that the proposed equations (Diep et al., 2022) underestimated the flexural moment strength by approximately (13.99 & 14.55) %, respectively. The flexural performance of the prefabricated composite girder was ensured. Therefore, it is recommended to use UHPC level

grouts, which have a high shear strength proven in many studies for the NC specimen. These results are in good agreement with the research results and design proposals of the FHWA research report (Graybeal, 2012).

**Table 1** The flexural moment strength comparison results

Parameters		$M_n$ (kNm)	$M_{FEA}$ (kNm)	Difference (%)
The concrete compressive strength (MPa)	20	2,615.73	3,243.90	19.36
	25	2,760.00	3,273.46	15.69
	30	2,945.19	3,292.33	10.54
	35	3,122.88	3,305.67	5.53
The grout compressive strength (MPa)	40	2,540.39	3,247.87	21.78
	60	2,589.51	3,292.93	21.36
	80	2,682.63	3,387.26	20.80
	100	2,756.43	3,410.00	19.17
The thickness of upper flange (mm)	14	2,562.82	3,287.38	22.04
	18	2,598.60	3,331.84	22.01
	22	2,633.05	3,369.95	21.87
The thickness of bottom flange (mm)	14	2,239.10	2,931.60	23.62
	22	2,777.13	3,536.32	21.47
	26	3,023.03	3,813.36	20.73
The height of steel girder (mm)	600	1,950.26	2,600.66	25.01
	850	2,956.63	3,806.50	22.33
	950	3,406.50	4,433.20	23.16
CC Specimen (Original Case)		2,531.41	3,218.83	21.36

**Fig. 11** The moment ratio–displacement curve

## 7 Conclusion

In this study, the flexural performance of the prefabricated composite girder was investigated. Test and finite element analysis of two test specimens were carried out. Parametric studies were then performed. From the results, the following conclusions were drawn:

(1) For the CC specimen: There was no failure in the connection interfaces at the ultimate loading state, and the flexural performance of the prefabricated composite girder with conventional precast deck-to-girder continuous connection was ensured. From this, the AASHTO

LRFD appears applicable to the existing conventional connection details.

- (2) For the NC specimen: Failure occurred at the monolithic grout interface. In particular, it is the shear plane corresponding to the minimum shear strength of the monolithic grout interfaces that is consistent with the connection design calculation theory. This non-intersected connection type influences the flexural moment strength and also the structural ductility, which is the rotation capacity, is more serious than the conventional connection type. Therefore, for the NC specimen, it is recommended to use UHPC level grouts, which have a high shear strength proven in many studies.
- (3) The investigated parameters have an effect on the flexural moment strength of the prefabricated composite girder. The compressive strength of concrete and grout, and the thickness of upper flange influence the flexural moment strength to a certain degree. Higher steel girder enhances the flexural moment strength efficiently. Compared with altering the height of steel girder, changing the thickness of bottom flange is considered as an easier method to improve the flexural moment strength within a certain range.
- (4) The flexural performance of the prefabricated composite girder was evaluated in this study, which shows that it was ensured with the appropriate design of connection details. Definitely, the structural ductility through the rotation capacity of the composite girder with the conventional connection design should be verified. It is desirable that a rational design method or correlation should be presented to readily meet the structural duc-

tility and rotation capacity required for flexural members through future further studies.

**Funding** This research was conducted with the support of the National R&D Project for Smart Construction Technology (Grant No.22 SMIP-A158708-03), funded by the Korea Agency for Infrastructure Technology Advancement under the Ministry of Land, Infrastructure and Tr

## References

- AASHTO LRFD Bridge Design Specifications, 9th Edition (2020).
- ABAQUS (2020). ABAQUS analysis user's guide.
- Abu-Tair, A. I., Rigden, S. R., & Burley, E. (1996). Testing the bond between repair materials and concrete substrate. *ACI Materials Journal*, 93(6), 553–558.
- Badie, S. S., Girgis, A., Tadros, M. K., & Nguyen, N. T. (2010). Relaxing the stud spacing limit for full-depth precast concrete deck panels supported on steel girders (phase I). *Journal of Bridge Engineering*, 15(5), 482–492.
- Baltay, P., & Gjelsvik, A. (1990). Coefficient of friction for steel on concrete at high normal stress. *Journal of Materials in Civil Engineering*, 2(1), 46–49.
- Biswas, M. (1986). Precast bridge deck design systems. *PCI Journal*, 31(2), 40–94.
- Chen, W. F. (1982). *Plasticity in reinforced concrete*. McGraw-Hill.
- Cho, J., Moon, J., Ko, H. J., & Lee, H. E. (2018). Flexural strength evaluation of concrete-filled steel tube (CFST) composite girder. *Journal of Constructional Steel Research*, 151, 12–24.
- Diep, H. T., & Choi, B. H. (2023). Shear transfer resistance with different interface conditions: Evaluation of design provisions and proposed equation. *Applied Sciences*, 13(14), 8203.
- Diep, H. T., Jang, M., Moon, J., & Choi, B. H. (2022). Numerical analysis on plastic moment capacity of prefabricated steel girders with injection channel connections. *International Journal of Steel Structures*, 22(6), 1722–1733.
- Diep, H. T., Moon, J., & Choi, B. H. (2023). Structural performance of prefabricated composite girders for railway bridges along with girder-to-deck interface connections for mechanical injection. *Applied Sciences*, 13(11), 6686.
- De La Varga, I., Haber, Z., and Graybeal, B. (2017). Bond of field-cast grouts to precast concrete elements. Report no. FHWA-HRT-16–081, FHWA-Federal Highway Administration, Washington, DC, USA.
- Graybeal, B. (2012). Ultra-high performance concrete composite connections for precast concrete bridge decks. Report no. FHWA-HRT-12–041, FHWA-Federal Highway Administration, Washington, DC, USA.
- Haber, Z. and Graybeal, B. (2018). Performance of grouted connections for prefabricated bridge deck elements. Report no. FHWA-HIF-19–003, FHWA-Federal Highway Administration, Washington, DC, USA.
- Hognestad, E. (1951). *A study of combined bending and axial load in reinforced concrete members*, Bulletin 399. University of Illinois Engineering Experiment Station.
- Kaushik, H. B., Rai, D. C., & Jain, S. K. (2007). Stress-strain characteristic of clay brick masonry under uniaxial compression. *Journal of Materials in Civil Engineering*, 19(9), 728–739.
- Momayez, A., Ehsani, M. R., Ramezani pour, A. A., & Rajaie, H. (2005). Comparison of methods for evaluating bond strength between concrete substrate and repair materials. *Cement and Concrete Research*, 35(4), 748–757.
- Oehlers, D. J., & Bradford, M. A. (1995). *Composite steel and concrete structural members: Fundamental behaviour*. Oxford: Pergamon Press.
- Ovuoba, B., & Prinz, G. S. (2018). Headed shear stud fatigue demands in composite bridge girders having varied stud pitch, girder depth, and span length. *Journal of Bridge Engineering*, 23(11), 04018085.
- Santos, P. M. D., Júlio, E. N. B. S., & Silva, V. D. (2007). Correlation between concrete-to-concrete bond strength and the roughness of the substrate surface. *Construction and Building Materials*, 21(8), 1688–1695.
- Tawadrous, R., & Morcou, G. (2018). Interface shear resistance of clustered shear connectors for precast concrete bridge deck systems. *Engineering Structures*, 160, 195–211.
- Zhu, P., & Ma, Z. J. (2010). Selection of durable closure pour materials for accelerated bridge construction. *Journal of Bridge Engineering*, 15(6), 695–704.

**Publisher's Note** Springer Nature remains neutral with regard to jurisdictional claims in published maps and institutional affiliations.

Springer Nature or its licensor (e.g. a society or other partner) holds exclusive rights to this article under a publishing agreement with the author(s) or other rightsholder(s); author self-archiving of the accepted manuscript version of this article is solely governed by the terms of such publishing agreement and applicable law.